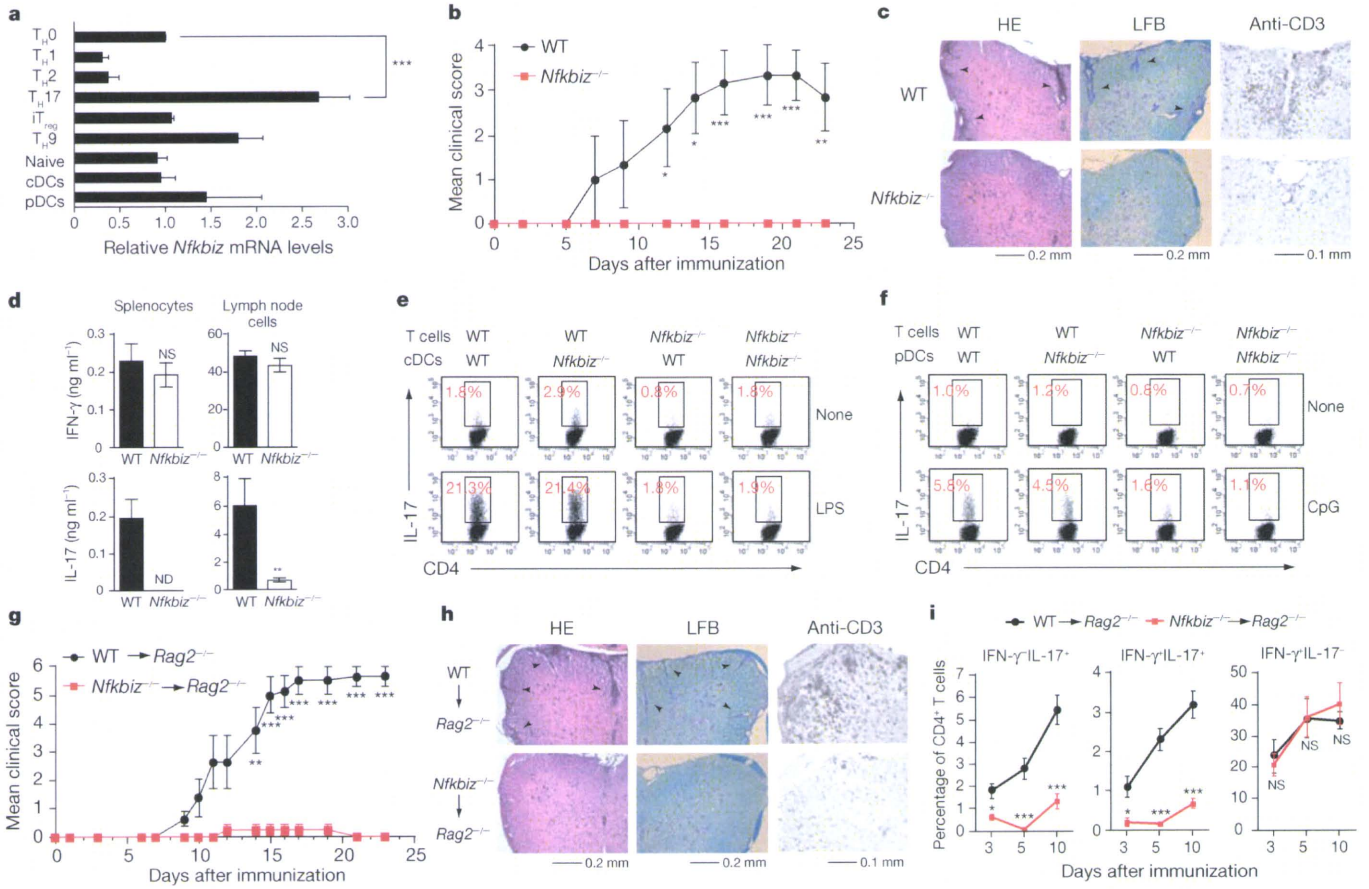

Figure 1 | *Nfkbiz*$^{-/-}$ mice are resistant to EAE owing to a CD4$^+$ T-cell-intrinsic defect in T_H17 development. **a**, *Nfkbiz* mRNA expression in T_H-cell subsets, inducible T_{reg} (iT_{reg}) cells, naive CD4$^+$ T cells (Naive), conventional dendritic cells (cDCs) and plasmacytoid DCs (pDCs). **b**, Disease course of EAE in wild-type (WT; $n = 5$) or *Nfkbiz*$^{-/-}$ mice ($n = 5$). **c**, Pathology analysis of the spinal cord sections. Arrowheads indicate inflammatory cellular infiltrate (haematoxylin and eosin, HE) and demyelinated areas (Luxol fast blue, LFB). **d**, IFN-γ and IL-17 production in splenocytes and lymph node cells after restimulation with MOG peptide. ND, not detected. **e**, **f**, TLR-induced IL-17 production in CD4$^+$ T cells in co-culture with cDCs (**e**) or pDCs (**f**) isolated from WT or *Nfkbiz*$^{-/-}$ mice. **g**, Disease course of EAE in *Rag2*$^{-/-}$ mice reconstituted with WT ($n = 8$) or *Nfkbiz*$^{-/-}$ ($n = 5$) CD4$^+$ T cells. **h**, Pathology analysis of the spinal cord sections from the reconstituted mice. **i**, Frequency of IFN-γ$^+$IL-17$^+$, IFN-γ$^-$IL-17$^+$ and IFN-γ$^+$IL-17$^-$ CD4$^+$ T cells in the reconstituted mice. Error bars (**a**, **b**, **d**, **g** and **i**), mean ± s.e.m.; $*P < 0.05$; $**P < 0.01$; $***P < 0.005$; NS, not significant.

which are related to T_H17 development[7,14–18], was normal in *Nfkbiz*$^{-/-}$ T cells (Supplementary Fig. 5). The expression of genes related to the migration of T_H17 cells (*Ccr6*, *Ccl20* and *S1pr1*)[2,3] and T_H17-related cytokine receptors (*Il6ra*, *Il6st*, *Il21r*, *Il2rg*, *Il1r1* and *Il1rap*), and IL-6-induced STAT3 phosphorylation, were also normal in *Nfkbiz*$^{-/-}$ T cells (Supplementary Figs 5 and 6). There was no defect in the generation of CD4$^+$CD25$^+$Foxp3$^+$ natural regulatory T (T_{reg}) cells in *Nfkbiz*$^{-/-}$ mice or the *in vitro* development of Foxp3-expressing T_{reg} cells from *Nfkbiz*$^{-/-}$ naive CD4$^+$ T cells (Supplementary Fig. 7). Taken together, IκBζ actively contributes to T_H17 development without affecting T_{reg} cell development.

IκBζ has three alternative splicing variants[10]: IκBζ (L) is the major splicing variant in macrophages, and IκBζ (S) lacks the amino-terminal 99 amino acids of IκBζ (L). Unlike these two variants, the minor splicing variant IκBζ (D) lacks transactivation activity[19]. Immunoblot and PCR with reverse transcription (RT–PCR) analyses showed that T_H17 cells predominantly expressed IκBζ (L) and slightly IκBζ (S), but not IκBζ (D) (Fig. 2e and Supplementary Figs 8 and 9).

IκBζ expression was upregulated by the combination of IL-6 and TGF-β, whereas IL-6 or TGF-β alone had no effect (Fig. 2f and Supplementary Figs 8 and 9). Addition of IL-23 did not have any effect on IκBζ expression (Fig. 2f and Supplementary Fig. 9b). IκBζ expression is regulated by the MyD88-mediated pathway in macrophages[11], and its mRNA is stabilized by the IL-17R-mediated signal in fibroblasts[20]. However, IκBζ is normally induced by the combination of IL-6 and TGF-β in *Myd88*$^{-/-}$ CD4$^+$ T cells, as well as in *Il17a*$^{-/-}$ CD4$^+$ T cells (Fig. 2g and Supplementary Fig. 9d). Notably, IκBζ induction was normal in *Rorc*$^{-/-}$ CD4$^+$ T cells, but severely impaired in Stat3-deficient CD4$^+$ T cells during T_H17 development (Fig. 2g and Supplementary Fig. 9d). Therefore, IκBζ induction is mediated by Stat3, but not by RORγt, in T_H17 cells.

We next investigated the mechanism by which IκBζ regulates T_H17 development. Overexpression of IκBζ in CD4$^+$ T cells induced T_H17 development only when stimulated with IL-6 and TGF-β (Fig. 3a, b and Supplementary Fig. 10), indicating that IκBζ does not act alone, but rather, cooperates with other factor(s) in T_H17 development. Among the T_H17-related cytokines, *Il22* expression was not upregulated by the overexpression of IκBζ without the addition of IL-23 (data not shown). We next determined which domain is responsible for IκBζ function in T_H17 development using IκBζ variants and deletion mutants[19] (Fig. 3c). IκBζ (L) and IκBζ (S) augmented T_H17 development significantly (Fig. 3d), but this augmentation was abolished in IκBζ (D) and IκBζ (L) 457–728, both of which lack the transcriptional activation domain (TAD), as well as in IκBζ (L) 1–456, which lacks the ARD (Fig. 3d). These results indicate that the function of IκBζ in T_H17 cells is dependent on both its transcriptional activity and ARD-mediated interaction with NF-κB.

The interaction between NF-κB p50 (encoded by the *Nfkb1* gene) and IκBζ is necessary for TLR-mediated induction of the inflammatory genes in macrophages[11]. This led us to examine whether p50 is required for IκBζ-mediated T_H17 development. p50 and RelA, but not cRel,

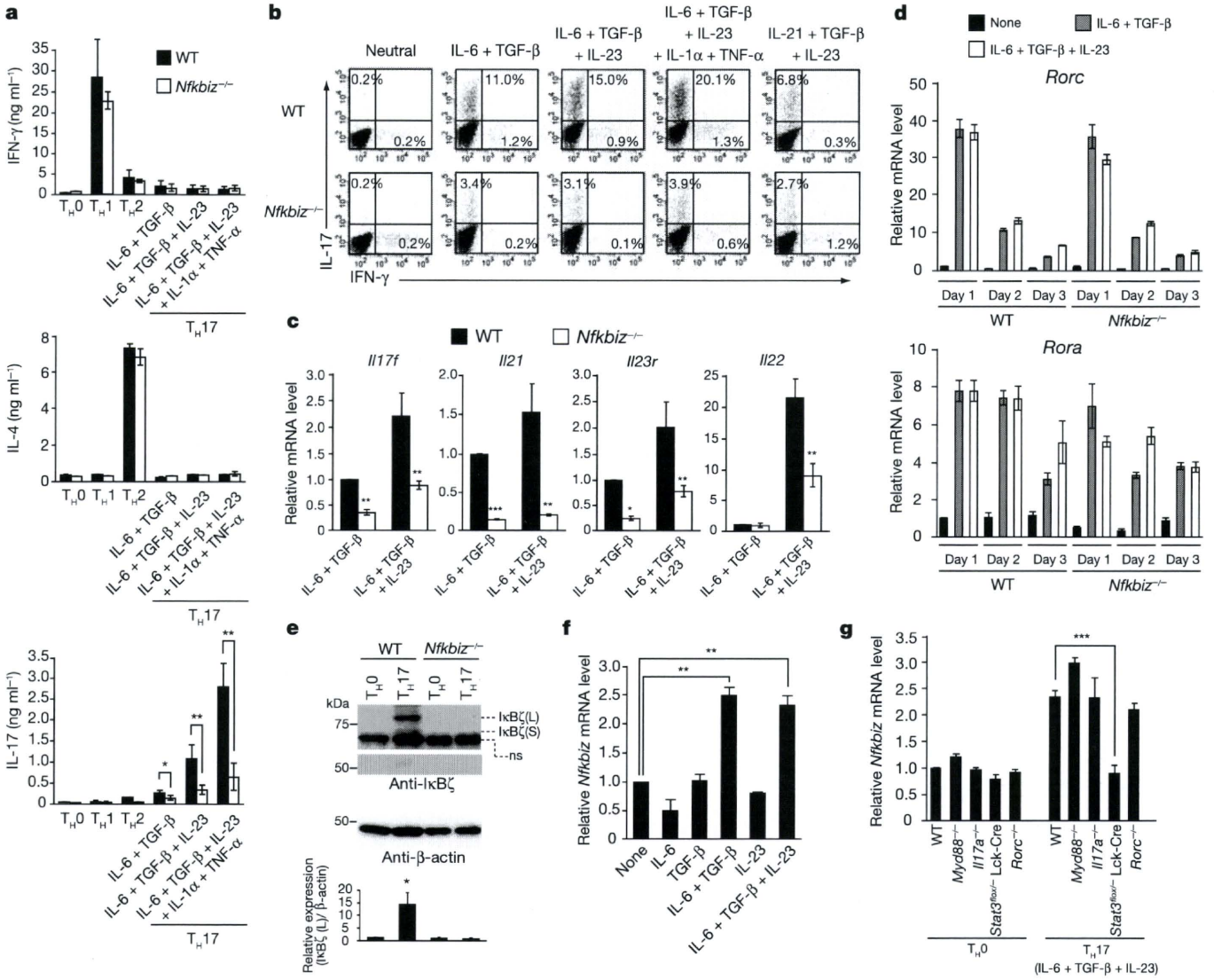

Figure 2 | Targeted disruption of the *Nfkbiz* gene results in impaired T_H17 development. **a**, IFN-γ, IL-4 and IL-17 production in WT or *Nfkbiz*$^{-/-}$ $CD4^+$ T cells activated under T_H0-, T_H1-, T_H2- or T_H17-polarizing conditions. **b**, Intracellular expression of IFN-γ and IL-17 in WT or *Nfkbiz*$^{-/-}$ $CD4^+$ T cells activated under T_H0- or T_H17-polarizing conditions. **c**, *Il17f*, *Il21*, *Il23r* and *Il22* mRNA expression in WT or *Nfkbiz*$^{-/-}$ $CD4^+$ T cells. **d**, *Rorc* and *Rora* mRNA expression in WT or *Nfkbiz*$^{-/-}$ $CD4^+$ T cells cultured for 1, 2 or 3 days. **e**, Protein expression level of the IκBζ splicing variants IκBζ (L) (79 kDa), IκBζ (S) (69 kDa) and IκBζ (D) (57 kDa) in T_H0 or T_H17 cells. ns, non-specific band. **f**, Effects of the cytokines on *Nfkbiz* mRNA expression in $CD4^+$ T cells. **g**, *Nfkbiz* mRNA expression in $CD4^+$ T cells derived from *Myd88*$^{-/-}$, *Il17a*$^{-/-}$, *Stat3*$^{flox/-}$ Lck-Cre or *Rorc*$^{-/-}$ mice. Error bars (**a** and **c**–**g**), mean ± s.e.m.; $*P < 0.05$; $**P < 0.01$; $***P < 0.005$.

enhanced the ability of IκBζ to induce IL-17 production under T_H17-polarizing conditions (Supplementary Fig. 11). However, *Nfkb1*$^{-/-}$ naive $CD4^+$ T cells normally differentiated into T_H17 cells (Supplementary Fig. 12), and ectopic expression of IκBζ enhanced T_H17 development even in *Nfkb1*$^{-/-}$ T cells (Supplementary Fig. 13). Therefore, p50 is not essential for IκBζ-mediated regulation of T_H17 development. In the absence of IL-6 and TGF-β, co-expression of IκBζ and an NF-κB subunit did not induce T_H17 development (Supplementary Fig. 11), indicating that a factor(s) other than NF-κB is required for IκBζ-mediated regulation of T_H17 development.

These results prompted us to test whether IκBζ functions in cooperation with RORγt or RORα in T_H17 development. In the absence of IL-6 and TGF-β, neither the ROR nuclear receptors nor IκBζ induced T_H17 development efficiently (Figs 3a and 4a), but when IκBζ (L) or (S) was overexpressed, either RORγt or RORα strongly induced IL-17 production, even in the absence of exogenous polarizing cytokines (Fig. 4a and Supplementary Fig. 14). These findings indicate that the ROR nuclear receptors and IκBζ synergistically promote T_H17 development. Under T_H17-polarizing conditions, RORγt or RORα alone strikingly induced IL-17 production (Fig. 4a), to which IκBζ induced by the combination of IL-6 and TGF-β may contribute (Fig. 2f and Supplementary Figs 8 and 9). IL-17 production induced by RORγt or RORα overexpression was significantly decreased in *Nfkbiz*$^{-/-}$ T cells under T_H17-polarizing conditions (Fig. 4b), the decrease of which was not restored by the addition of exogenous IL-21 or IL-9 (Supplementary Fig. 15). IL-17 induction was severely impaired when IκBζ was overexpressed in *Rorc*$^{-/-}$ or homozygous *Staggerer* mutation (*Rora*$^{sg/sg}$) cells[21] (Fig. 4c and Supplementary Fig. 16). Taken together, the cooperation of IκBζ with RORγt or RORα is clearly essential for T_H17 development.

Does IκBζ directly regulate the *Il17a* promoter? Seven IκBζ response elements[22] were found within the 6.6-kilobase-pair promoter region of the mouse *Il17a* gene (Fig. 4d). The reporter assay showed that IκBζ (L) and (S) moderately activated the *Il17a* promoter as well as RORγt and RORα (Fig. 4e). When RORγt or RORα was expressed, IκBζ (L) and (S), but not (D), activated the *Il17a* promoter to a much larger extent (Fig. 4e). An evolutionarily conserved non-coding sequences (CNS) 2 region in the *Il17a* locus was reported to be associated with histone H3 acetylation in a T_H17 lineage-specific

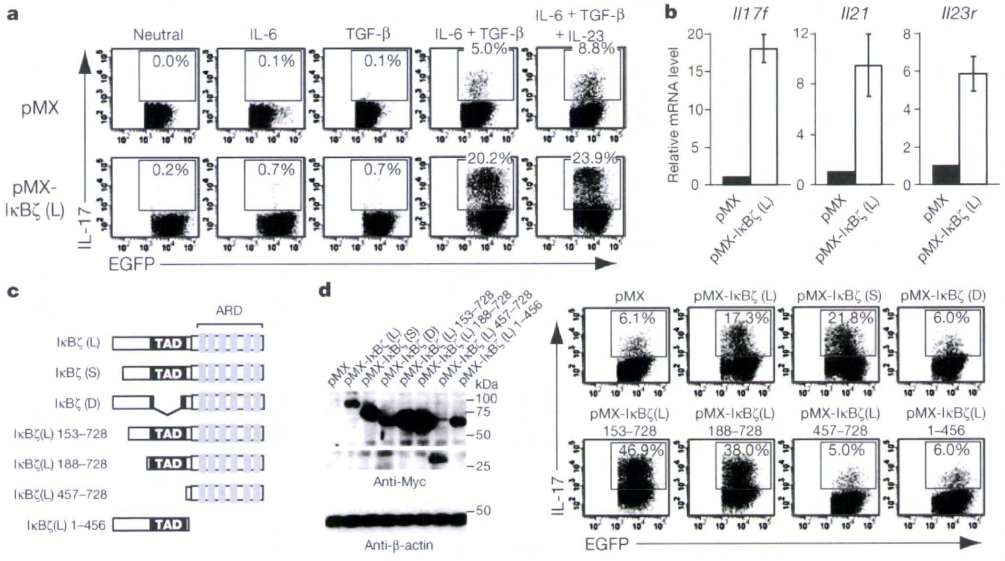

Figure 3 | Ectopic expression of IκBζ facilitates T_H17 development. **a**, Effects of retroviral expression of IκBζ (L) on IL-17 production. **b**, Effects of retroviral expression of IκBζ (L) on *Il17f*, *Il21* and *Il23r* mRNA expression in $CD4^+$ T cells activated in the presence of IL-6 and TGF-β. Error bars, mean ± s.e.m. **c**, Schematic of IκBζ variants and truncated mutants of IκBζ (L). **d**, Effects of retroviral expression of the Myc-tagged IκBζ variants and mutants on T_H17 development (right). Immunoblot analysis of IκBζ protein levels in Myc-tagged IκBζ variants-expressing $CD4^+$ T cells (left). IκBζ (L) 153–728 and IκBζ (L) 188–728 had a more potent activity to induce IL-17 production than IκBζ (L), which may be correlated to their high expression levels.

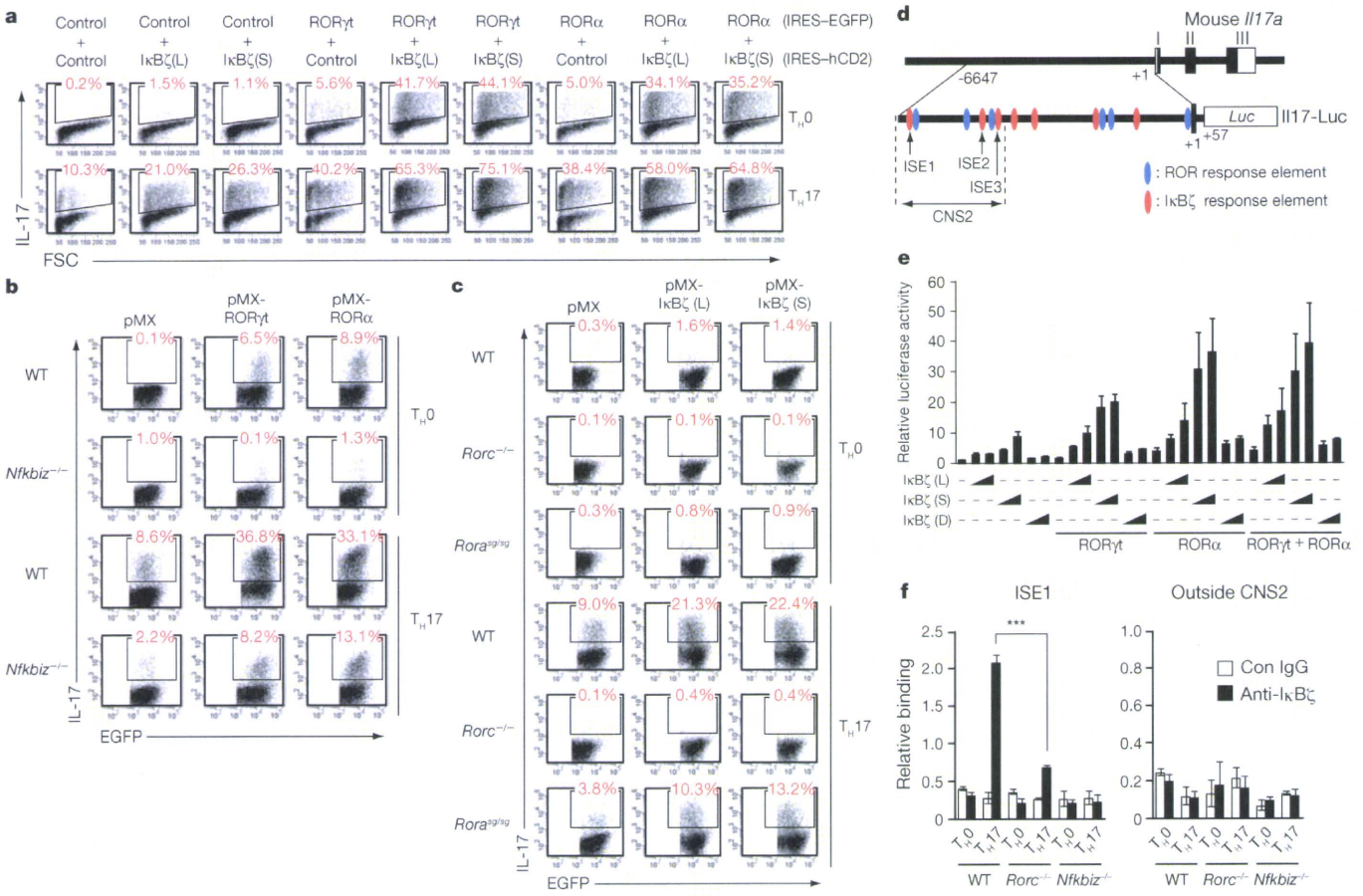

Figure 4 | IκBζ and ROR nuclear receptors cooperatively activate the *Il17a* promoter and facilitate T_H17 development. **a**, IL-17 production in $CD4^+$ T cells transduced with IκBζ (IRES–hCD2) and RORγt or RORα (IRES–EGFP) after activation under T_H0- or T_H17-polarizing conditions. FSC, forward scatter. **b**, Effects of retroviral expression of RORγt or RORα on IL-17 production in WT or *Nfkbiz*$^{-/-}$ $CD4^+$ T cells. **c**, Effects of retroviral expression of IκBζ on IL-17 production in WT, *Rorc*$^{-/-}$ or *Rora*$^{sg/sg}$ $CD4^+$ T cells. **d**, Putative IκBζ and ROR response elements[5,17,21] in the mouse *Il17a* promoter and the Il17-Luc construct. Three IκBζ response elements were located in the CNS2 region (ISE1, −6350 to −6339; ISE2, −4795 to −4786; ISE3, −4454 to −4445). The transcriptional initiation site was designated as +1. **e**, Effects of IκBζ on RORγt and/or RORα-mediated activation of the *Il17a* promoter. **f**, Recruitment of IκBζ to the ISE1 region or the region outside CNS2 (−3978 to −3969) in WT, *Rorc*$^{-/-}$, *Nfkbiz*$^{-/-}$ $CD4^+$ T cells. Error bars (**e** and **f**), mean ± s.e.m. ***$P < 0.005$.

manner and with ROR nuclear receptor-directed IL-17 production[5,17,23]. IκBζ facilitated the CNS2 enhancer activity in combination with RORγt and RORα (Supplementary Fig. 17a, b). However, the *Il17a* promoter region lacking the CNS2 region was not activated by the co-expression of IκBζ and RORγt or RORα (Supplementary Fig. 17a, c, d). IκBζ induced the CNS2 enhancer activity mainly through the distal IκBζ response element (ISE1: −6350 to −6339) (Fig. 4d) among the three IκBζ response elements in the CNS2 region (Supplementary Fig. 18). Chromatin immunoprecipitation (ChIP) experiments showed that IκBζ was recruited to the ISE1 region in T_H17 cells, but not in T_H0 cells (Fig. 4f). We observed no physical interaction between IκBζ and RORγt or RORα by immunoprecipitation assay (data not shown), but recruitment of IκBζ to the ISE1 region was dependent on RORγt (Fig. 4f). These results indicate that T_H17 development entails IκBζ recruitment to the regulatory region of the *Il17a* gene, a process in which ROR nuclear receptors have a critical role.

This study demonstrates that IκBζ, which has a key role in the innate immune response, regulates T_H17 development in a T-cell-intrinsic manner. IκBζ, like Runx1 and Batf[14,17], does not act alone, but in cooperation with ROR nuclear receptors. This does not reduce the importance of IκBζ as the therapeutic target, because disruption of IκBζ alone leads to a complete resistance to EAE (Fig. 1). Runx1, Batf and IRF4 function upstream of RORγt[7,14,17], but it is unlikely that ROR nuclear receptors function downstream of IκBζ or vice versa (Fig. 2d, g and Supplementary Fig. 9d). We speculate that the binding of both IκBζ and ROR nuclear receptors to the *Il17* promoter leads to an efficient recruitment of transcriptional coactivators with histone acetylase activity[5,23]. Moreover, RORγt may be involved in the regulation of the accessibility of IκBζ to the specific transcriptional regulatory regions (Fig. 4f). Interestingly, *Il17f*, *Il21* and *Il23r* mRNA expression was impaired in *Nfkbiz*$^{-/-}$ T cells (Fig. 2c). ChIP analyses showed recruitment of IκBζ to the promoter or the enhancer region of these T_H17-related cytokine genes (Supplementary Fig. 19), indicating that IκBζ directly regulates these genes. *Nfkbiz*$^{-/-}$ mice develop atopic dermatitis-like skin lesions[11,24]. However, as the dermatitis was not observed in the *Rag2*$^{-/-}$ mice reconstituted with *Nfkbiz*$^{-/-}$ CD4$^+$ T cells or *Nfkbiz*$^{-/-}$ fetal liver cells (data not shown), it is not likely that the dermatitis was caused by T-cell-intrinsic abnormalities, including impaired T_H17 development. Thus, the present study demonstrates the T-cell-specific function of IκBζ, which is important for understanding the transcriptional program in T_H17 cell lineage commitment.

METHODS SUMMARY

T-cell differentiation *in vitro*. Naive CD4$^+$ T cells were purified from spleen using the CD4$^+$CD62L$^+$ T Cell Isolation Kit (Miltenyi Biotec) (purity was >95%) and activated with plate-bound 2 μg ml^{-1} anti-CD3 (145-2C11, BD Biosciences) and 2 μg ml^{-1} anti-CD28 (37.51, BD Biosciences) for 3 days under various polarizing conditions (see Methods for details).

Full Methods and any associated references are available in the online version of the paper at www.nature.com/nature.

Received 12 August 2009; accepted 10 February 2010.
Published online 11 April 2010.

1. Korn, T., Bettelli, E., Oukka, M. & Kuchroo, V. K. IL-17 and Th17 cells. *Annu. Rev. Immunol.* **27,** 485–517 (2009).
2. Dong, C. T_H17 cells in development: an updated view of their molecular identity and genetic programming. *Nature Rev. Immunol.* **8,** 337–348 (2008).
3. O'Shea, J. J. *et al.* Signal transduction and Th17 cell differentiation. *Microbes Infect.* **11,** 599–611 (2009).
4. Ivanov, I. I. *et al.* The orphan nuclear receptor RORγt directs the differentiation program of proinflammatory IL-17$^+$ T helper cells. *Cell* **126,** 1121–1133 (2006).
5. Yang, X. O. *et al.* T helper 17 lineage differentiation is programmed by orphan nuclear receptors RORα and RORγ. *Immunity* **28,** 29–39 (2008).
6. Manel, N., Unutmaz, D. & Littman, D. R. The differentiation of human T_H-17 cells requires transforming growth factor-β and induction of the nuclear receptor RORγt. *Nature Immunol.* **9,** 641–649 (2008).
7. Brüstle, A. *et al.* The development of inflammatory T_H-17 cells requires interferon-regulatory factor 4. *Nature Immunol.* **8,** 958–966 (2007).
8. Huber, M. *et al.* IRF4 is essential for IL-21-mediated induction, amplification, and stabilization of the Th17 phenotype. *Proc. Natl Acad. Sci. USA* **105,** 20846–20851 (2008).
9. Yamazaki, S., Muta, T. & Takeshige, K. A novel IκB protein, IκB-ζ, induced by proinflammatory stimuli, negatively regulates nuclear factor-κB in the nuclei. *J. Biol. Chem.* **276,** 27657–27662 (2001).
10. Muta, T. IκB-ζ: an inducible regulator of nuclear factor-κB. *Vitam. Horm.* **74,** 301–316 (2006).
11. Yamamoto, M. *et al.* Regulation of Toll/IL-1-receptor-mediated gene expression by the inducible nuclear protein IκBζ. *Nature* **430,** 218–222 (2004).
12. Yamamoto, M. & Takeda, K. Role of nuclear IκB proteins in the regulation of host immune responses. *J. Infect. Chemother.* **14,** 265–269 (2008).
13. Veldhoen, M., Hocking, R. J., Atkins, C. J., Locksley, R. M. & Stockinger, B. TGFβ in the context of an inflammatory cytokine milieu supports de novo differentiation of IL-17-producing T cells. *Immunity* **24,** 179–189 (2006).
14. Schraml, B. U. *et al.* The AP-1 transcription factor Batf controls T_H17 differentiation. *Nature* **460,** 405–409 (2009).
15. Quintana, F. J. *et al.* Control of T_{reg} and T_H17 cell differentiation by the aryl hydrocarbon receptor. *Nature* **453,** 65–71 (2008).
16. Veldhoen, M. *et al.* The aryl hydrocarbon receptor links T_H17-cell-mediated autoimmunity to environmental toxins. *Nature* **453,** 106–109 (2008).
17. Zhang, F., Meng, G. & Strober, W. Interactions among the transcription factors Runx1, RORγt and Foxp3 regulate the differentiation of interleukin 17-producing T cells. *Nature Immunol.* **9,** 1297–1306 (2008).
18. Chen, Z. *et al.* Selective regulatory function of Socs3 in the formation of IL-17-secreting T cells. *Proc. Natl Acad. Sci. USA* **103,** 8137–8142 (2006).
19. Motoyama, M., Yamazaki, S., Eto-Kimura, A., Takeshige, K. & Muta, T. Positive and negative regulation of nuclear factor-κB-mediated transcription by IκB-ζ, an inducible nuclear protein. *J. Biol. Chem.* **280,** 7444–7451 (2005).
20. Yamazaki, S., Muta, T., Matsuo, S. & Takeshige, K. Stimulus-specific induction of a novel nuclear factor-κB regulator, IκB-ζ, via Toll/interleukin-1 receptor is mediated by mRNA stabilization. *J. Biol. Chem.* **280,** 1678–1687 (2005).
21. Jetten, A. M. & Joo, J. H. Retinoid-related orphan receptors (RORs): roles in cellular differentiation and development. *Adv. Dev. Biol.* **16,** 313–355 (2006).
22. Matsuo, S., Yamazaki, S., Takeshige, K. & Muta, T. Crucial roles of binding sites for NF-κB and C/EBPs in IκB-ζ-mediated transcriptional activation. *Biochem. J.* **405,** 605–615 (2007).
23. Akimzhanov, A. M., Yang, X. O. & Dong, C. Chromatin remodeling of interleukin-17 (IL-17)-IL-17F cytokine gene locus during inflammatory helper T cell differentiation. *J. Biol. Chem.* **282,** 5969–5972 (2007).
24. Shiina, T. *et al.* Targeted disruption of MAIL, a nuclear IκB protein, leads to severe atopic dermatitis-like disease. *J. Biol. Chem.* **279,** 55493–55498 (2004).

Supplementary Information is linked to the online version of the paper at www.nature.com/nature.

Acknowledgements We are grateful to Y. Iwakura and T. Kitamura for providing *Il17a*$^{-/-}$ mice and retrovirus vectors, respectively. We also thank M. Shinohara, T. Negishi-Koga, M. Asagiri, T. Nakashima, N. Komatsu, M. Ohba, Y. Kunisawa, Y. Suzuki, S. Miyakoshi and T. Kunigami for discussion and assistance. This work was supported in part by Grant-in-Aid for Creative Scientific Research from the Japan Society for the Promotion of Science (JSPS), Grant-in-Aid for Challenging Exploratory Research from JSPS, Grant-in-Aid for JSPS Fellows, Grants-in-Aid for GCOE Program from the Ministry of Education, Culture, Sports, Science and Technology of Japan (MEXT), and ERATO, Takayanagi Osteonetwork Project from JST. It was also supported by grants from the Intramural Research Program of the NIEHS (Z01-ES-101586) (to A.M.J.), Takeda Life Science Foundation and Yokoyama Foundation for Clinical Pharmacology and the Ichiro Kanehara Foundation. Ka.O. is supported by JSPS Research Fellowships for Young Scientists.

Author Contributions Ka.O. performed all of the experiments, interpreted the results and prepared the manuscript. Y.I. contributed to dendritic cells experiments and T-cell transfer experiments. M.O. contributed to study design and manuscript preparation. M.Y., A.M.J. and S.A. provided genetically modified mice and advice on data analysis. To.M. provided advice on project planning and data interpretation. K.A. and Ke.O. supported the experiments using *Nfkb1*$^{-/-}$ mice. Ta.M. provided genetically modified mice and the plasmids, and advised on project planning. H.T. directed the project and wrote the manuscript.

Author Information Reprints and permissions information is available at www.nature.com/reprints. The authors declare no competing financial interests. Correspondence and requests for materials should be addressed to H.T. (taka.csi@tmd.ac.jp).

METHODS

Mice. We used *Nfkbiz*$^{-/-}$ mice on a mixed 129Sv-C57BL/6 background at 5 weeks after birth[11] because of the almost complete embryonic lethality of the inbred C57BL/6 genetic background. *Rorc*$^{-/-}$ (ref. 25), *Myd88*$^{-/-}$ (ref. 26), and *Il17a*$^{-/-}$ (ref. 27) mice on a C57BL/6 background were described previously. *Nfkb1*$^{-/-}$ (ref. 28) and *Rora*$^{sg/+}$ (ref. 29) mice on a C57BL/6 background were obtained from The Jackson Laboratory. *Rag2*$^{-/-}$ mice on a C57BL/6 background were purchased from Taconic Farms. For the generation of mice with T-cell-specific disruption of *Stat3*, Lck-Cre transgenic mice (The Jackson Laboratory) were bred with *Stat3*$^{flox/-}$ mice[30]. We used wild-type littermates as controls in all experiments. All of the animals were maintained in a specific pathogen-free environment, and all animal experiments were performed with the approval of the institutional committee.

T-cell differentiation *in vitro*. The conditions for different T_H cell subsets were: 10 μg ml^{-1} anti-IL-4 (11B11, BD Biosciences) and 10 μg ml^{-1} anti-IFN-γ (XMG1.2, BD Biosciences) for T_H0 (neutral conditions); 10 μg ml^{-1} anti-IL-4 and 10 ng ml^{-1} IL-12 (PeproTech) for T_H1; 10 μg ml^{-1} anti-IFN-γ and 10 ng ml^{-1} IL-4 (PeproTech) for T_H2; 10 μg ml^{-1} anti-IL-4, 10 μg ml^{-1} anti-IFN-γ and 2.5 ng ml^{-1} TGF-β (PeproTech) for inducible T_{reg}; 10 μg ml^{-1} anti-IFN-γ, 10 ng ml^{-1} IL-4 and 1 ng ml^{-1} TGF-β for T_H9; 10 μg ml^{-1} anti-IL-4, 10 μg ml^{-1} anti-IFN-γ, 30 ng ml^{-1} IL-6 (PeproTech), 2.5 ng ml^{-1} TGF-β, 50 ng ml^{-1} IL-23 (R&D Systems), 80 ng ml^{-1} IL-21 (R&D Systems), 10 ng ml^{-1} IL-1α (PeproTech), 10 ng ml^{-1} TNF-α (R&D Systems) or a combination of these stimuli for T_H17. Activated cells were restimulated with 40 ng ml^{-1} phorbol-12-myristate-13-acetate (PMA) (Calbiochem) and 0.5 μg ml^{-1} ionomycin (Sigma-Aldrich) in the presence of GolgiPlug (BD Biosciences) for 4 h before intracellular staining, or restimulated with 2 μg ml^{-1} anti-CD3 and 2 μg ml^{-1} anti-CD28 for 3 days before enzyme-linked immunosorbent assay (ELISA). We cultured cells in RPMI 1640 medium (Invitrogen) unless otherwise indicated, or in IMDM medium (Sigma-Aldrich) in Supplementary Figs 8a, c and 9c.

Induction of EAE. The MOG35–55 peptide (MEVGWYRSPFSRVVHLYRNGK) was synthesized by Biologica. For the induction of EAE, we used 5-week-old *Nfkbiz*$^{-/-}$ mice in which no apparent symptoms of dermatitis were observed. Age-matched wild-type and *Nfkbiz*$^{-/-}$ mice were immunized subcutaneously with the MOG peptide (250 μg per mouse) emulsified in complete Freund's adjuvant (CFA) containing 40 ng ml^{-1} *Mycobacterium tuberculosis* H37RA (Difco Laboratories) (day 0). After immunization, the mice were intraperitoneally injected with pertussis toxin (200 ng per mouse, Sigma-Aldrich) on days 0 and 2. On day 23, lymphoid cells were prepared from the spleens and lymph nodes of the immunized mice, and were then stimulated with 25 μg ml^{-1} MOG peptide, or 2 μg ml^{-1} anti-CD3 and 2 μg ml^{-1} anti-CD28 for 48 h, after which IFN-γ and IL-17 production was analysed by ELISA.

For the induction of EAE in the reconstituted *Rag2*$^{-/-}$ mice, MOG peptide (150 μg per mouse) emulsified in CFA was injected on days 0 and 7. Pertussis toxin (400 ng per mouse) was injected on days 1 and 8. On day 3, 5 or 10, splenocytes isolated from the recipients were stimulated with 2 μg ml^{-1} anti-CD3 and 2 μg ml^{-1} anti-CD28 for 24 h. GolgiPlug was added for the final 4 h of culture, and then intracellular IL-17 and IFN-γ expression in CD4$^+$ T cells was analysed by flow cytometry. For the 5-bromo-2′-deoxyuridine (BrdU) incorporation assay, the mice were intraperitoneally injected with BrdU (1 mg per mouse, Sigma-Aldrich) on day 10. Eighteen hours later, CD4$^+$ T cells isolated from the spleen were analysed by flow cytometry using fluorescein isothiocyanate (FITC)-conjugated anti-BrdU (3D4, BD Biosciences).

Animals were scored for clinical signs of EAE for 23 days using the following criteria: 0, no clinical signs; 1, limp tail (tail paralysis); 2, complete loss of tail tonicity or abnormal gait; 3, partial hind limb paralysis; 4, complete hind limb paralysis; 5, forelimb paralysis or moribund; and 6, death. Histological analyses were performed as described[31].

CD4$^+$ T-cell transfer. CD4$^+$ T cells were prepared from the spleens of wild-type and *Nfkbiz*$^{-/-}$ mice using the CD4$^+$ T Cell Isolation Kit (Miltenyi Biotec) (purity was >95%). CD4$^+$ T cells (7×10^6 per mouse) were injected intravenously into *Rag2*$^{-/-}$ mice. One day later, the recipient mice were subjected to EAE induction.

Purification of dendritic cells and dendritic cell–T cell co-culture. PDCA1$^+$ cells and PDCA1$^-$CD11c$^+$ cells were used as plasmacytoid and conventional dendritic cells, respectively, which were isolated from the spleen using anti-PDCA1 microbeads and anti-CD11c microbeads (Miltenyi Biotec) (purity was >95%). In the presence of either 100 ng ml^{-1} lipopolysaccharide (LPS; Sigma-Aldrich) or 100 nM endotoxin-free phosphorothioate-stabilized CpG oligodeoxynucleotides (5′-TCCATGACGTTCCTGATGCT-3′) (Hokkaido System Science), naive CD4$^+$ T cells were co-cultured with dendritic cells in the presence of 1 ng ml^{-1} soluble anti-CD3, 2.5 ng ml^{-1} TGF-β, 10 μg ml^{-1} anti-IFN-γ and 10 μg ml^{-1} anti-IL-4. Three days later, cells were restimulated with 40 ng ml^{-1} PMA plus 0.5 μg ml^{-1} ionomycin in the presence of GolgiPlug for 4 h, after which CD4$^+$ T cells were analysed for intracellular IL-17 and IFN-γ. For analysis of cytokine production and surface marker expression, dendritic cells were cultured with 100 ng ml^{-1} LPS or 100 nM CpG DNA for 24 h.

Quantitative RT–PCR. Total RNA was extracted with ISOGEN (Wako). Quantitative RT–PCR was performed with a LightCycler (Roche) using SYBR Green (Toyobo) as described[31]. The primer sequences are described in Supplementary Table 1. The level of mRNA expression was normalized to that of *Gapdh* mRNA expression.

ELISA. Concentrations of cytokines in the culture supernatant were determined by ELISA kits (IFN-γ, IL-4 and IL-17, BD Biosciences; IL-6 and TNF-α, eBioscience), according to the manufacturers' instructions.

Retroviral transduction. pMX-IRES-EGFP and pMX-IRES-hCD2 are bicistronic retroviral vectors containing enhanced green fluorescence protein (EGFP) and human CD2 lacking the cytoplasmic domain, respectively, under the control of an internal ribosome entry site (IRES)[32]. The cDNA fragments of CD2, RORγt, RORα, RelA, cRel and p50 were amplified by PCR. cDNA fragments of IκBζ splicing variants and truncated mutants[19] were cloned into pMX-IRES-EGFP or pMX-IRES-hCD2 with a Myc tag added at its 5′ end. cDNA fragments of RORγt, RORα, RelA, cRel and p50 were cloned into pMX-IRES-EGFP. Retroviral packaging was performed by transfecting Plat-E cells with the plasmids as described previously[33]. Naive CD4$^+$ T cells were plated in wells pre-coated with 100 μg ml^{-1} goat anti-hamster IgG (Cappel) followed by 0.5 μg ml^{-1} anti-CD3 and 0.5 μg ml^{-1} anti-CD28 for 3 days in the presence of 5 ng ml^{-1} IL-2 (PeproTech) under the following conditions: anti-IL-4, anti-IFN-γ for T_H0 (neutral conditions); anti-IL-4, anti-IFN-γ, IL-6 and TGF-β for T_H17. In Supplementary Fig. 14, 10 μg ml^{-1} anti-TGF-β (1D11, R&D Systems) were added into the cultures. On days 1 and 2, cells were infected with fresh retroviral supernatant by centrifugation for 2 h at 780*g* in the presence of 10 μg ml^{-1} polybrene (Sigma-Aldrich). Cells were further cultured for 3 days. For intracellular cytokine staining, cells were restimulated for 4 h with 40 ng ml^{-1} PMA plus 0.5 μg ml^{-1} ionomycin in the presence of GolgiPlug. For quantitative RT–PCR and immunoblot analyses, EGFP$^+$ cells were sorted by MoFlo (Beckman Coulter).

Flow cytometry and antibodies. For the analysis of natural T_{reg} cells, single-cell suspensions prepared from the thymus, spleen and lymph nodes were stained with fluorophore-conjugated monoclonal antibodies: FITC-conjugated anti-CD4 (RM4-5, BD Biosciences), phycoerythrin-cyanine 7-conjugated anti-CD25 (PC61, BD Biosciences) and allophycocyanin-conjugated anti-Foxp3 (FJK-16 s, eBioscience). For intracellular cytokine staining, phycoerythrin-conjugated anti-mouse IL-17 (TC11-18H10, BD Biosciences), allophycocyanin-conjugated anti-mouse IFN-γ (XMG1.2, BD Biosciences) and allophycocyanin-conjugated anti-human CD2 (LFA-2, eBioscience) were used. For the analysis of the phosphorylation of STAT3, cells were stained with anti-phospho-STAT3 (D3A7, Cell Signaling Technology) followed by FITC-conjugated goat anti-rabbit IgG (BioSource). Flow cytometric analysis was performed by FACSCanto II with Diva software (BD Biosciences).

Reporter gene assay. The reporter plasmid Il17-Luc, Il17 4371-Luc and Il17 1547-Luc were constructed by subcloning a 6,647-base-pair (bp) fragment, a 4,371-bp fragment and a 1,547-bp fragment of the 5′ flanking region of the mouse *Il17a* gene, respectively, into the pGL3-basic vector (Promega). Il17 CNS2-Luc was constructed by subcloning the CNS2 region of the *Il17a* gene into the pTAL-Luc (Clontech). The mutations introduced into Il17 CNS2-Luc were as follows: 5′-AGGGACTGTCCC-3′ (ISE1) to 5′-AAATACTGTCCC-3′; 5′-GGGAAAACACT-3′ (ISE2) to 5′-AATAAAACACT-3′; 5′-GGAAGCGCCT-3′ (ISE3) to 5′-ATAAGCGCCT-3′. The expression plasmids of IκBζ (L), (S) and (D) have been described[19]. cDNA fragments of RORγt and RORα amplified by PCR were subcloned into the expression vector. The reporter plasmids and the expression plasmids were transfected into HEK293T cells using FuGENE 6 (Roche). After 36 h, dual luciferase assay was performed according to the manufacturer's protocol (Promega).

Immunoblot analysis. Immunoblot analysis was performed using antibodies against β-actin (Sigma-Aldrich), Myc (MBL) or IκBζ (C-15, Santa Cruz) as described[31].

Chromatin immunoprecipitation assay. Naive CD4$^+$ T cells were activated with plate-bound 2 μg ml^{-1} anti-CD3 and 2 μg ml^{-1} anti-CD28 for 3 days in the presence of anti-IL-4 and anti-IFN-γ for the development of T_H0, or anti-IL-4, anti-IFN-γ, IL-6, TGF-β and IL-23 for the development of T_H17. ChIP assay was performed using antibodies against IκBζ (C-15, Santa Cruz) and normal goat IgG (Santa Cruz) as described with minor modifications[34]. Quantitative PCR was performed with a LightCycler using the primers described in Supplementary Table 2. The data are presented as the relative binding based on normalization to input DNA. The evolutionarily conserved regions were identified as regions sharing at least 70% sequence identity across at least 100 bp using the rVista 2.0 web tool[35].

Statistical analysis. All data are expressed as the mean ± s.e.m. ($n = 3$ or more). Statistical analysis was performed using the unpaired two-tailed Student's *t*-test

($^{*}P < 0.05$; $^{**}P < 0.01$; $^{***}P < 0.005$; NS, not significant, throughout the paper). Results are representative examples of more than three independent experiments.

25. Kurebayashi, S. *et al.* Retinoid-related orphan receptor γ (RORγ) is essential for lymphoid organogenesis and controls apoptosis during thymopoiesis. *Proc. Natl Acad. Sci. USA* **97,** 10132–10137 (2000).
26. Adachi, O. *et al.* Targeted disruption of the MyD88 gene results in loss of IL-1- and IL-18-mediated function. *Immunity* **9,** 143–150 (1998).
27. Nakae, S. *et al.* Antigen-specific T cell sensitization is impaired in IL-17-deficient mice, causing suppression of allergic cellular and humoral responses. *Immunity* **17,** 375–387 (2002).
28. Sha, W. C., Liou, H. C., Tuomanen, E. I. & Baltimore, D. Targeted disruption of the p50 subunit of NF-κB leads to multifocal defects in immune responses. *Cell* **80,** 321–330 (1995).
29. Hamilton, B. A. *et al.* Disruption of the nuclear hormone receptor RORα in *staggerer* mice. *Nature* **379,** 736–739 (1996).
30. Takeda, K. *et al.* Stat3 activation is responsible for IL-6-dependent T cell proliferation through preventing apoptosis: generation and characterization of T cell-specific Stat3-deficient mice. *J. Immunol.* **161,** 4652–4660 (1998).
31. Asagiri, M. *et al.* Cathepsin K-dependent toll-like receptor 9 signaling revealed in experimental arthritis. *Science* **319,** 624–627 (2008).
32. Kitamura, T. *et al.* Retrovirus-mediated gene transfer and expression cloning: powerful tools in functional genomics. *Exp. Hematol.* **31,** 1007–1014 (2003).
33. Shinohara, M. *et al.* Tyrosine kinases Btk and Tec regulate osteoclast differentiation by linking RANK and ITAM signals. *Cell* **132,** 794–806 (2008).
34. Koga, T. *et al.* NFAT and Osterix cooperatively regulate bone formation. *Nature Med.* **11,** 880–885 (2005).
35. Loots, G. G. & Ovcharenko, I. rVISTA 2.0: evolutionary analysis of transcription factor binding sites. *Nucleic Acids Res.* **32,** W217–W221 (2004).

PEDIATRICS INTERNATIONAL Official Journal of the Japan Pediatric Society

Pediatrics International (2010) **52**, e196–e199 doi: 10.1111/j.1442-200X.2010.03135.x

Patient Report

Prominent eosinophilia but less eosinophil activation in a patient with Omenn syndrome

Mitsuru Seki,[1,2] Hirokazu Kimura,[3] Akio Mori,[4] Akira Shimada,[5] Yoshiyuki Yamada,[1] Kenichi Maruyama,[2] Yasuhide Hayashi,[5] Kazunaga Agematsu,[6] Tomohiro Morio,[7] Akihiro Yachie[8] and Masahiko Kato[1]

Departments of [1]*Allergy and Immunology,* [2]*Internal Medicine and* [5]*Hematology and Oncology, Gunma Children's Medical Center, Shibukawa, Gunma,* [3]*National Institute of Infectious Diseases, Musashimurayama,* [7]*Department of Pediatrics and Developmental Biology, Graduate School, Tokyo Medical and Dental University, Tokyo,* [4]*Department of Allergy, National Hospital Organization Sagamihara National Hospital, Sagamihara, Kanagawa,* [6]*Department of Pediatrics, Shinshu University Graduate School of Medicine, Matsumato, Nagano,* [8]*Angiogenesis and Vascular Development (Department of Pediatrics), Kanazawa University Graduate School of Medical Science, Kanazawa, Ishikawa, Japan*

Key words cytokines, eosinophils, immunodeficiency, Omenn syndrome.

Abbreviations: ECP, eosinophil cationic protein; GM-CSF, granulocyte-macrophage colony-stimulating factor; HES, hypereosinophilic syndrome; IFN, interferon; IL, interleukin; OS, Omenn syndrome; PBMC, peripheral blood mononuclear cells; PMA, phorbol 12-myristate 13-acetate; RAG, recombination activating genes; SCID, severe combined immunodeficiency; Th, T helper; TNF, tumor necrosis factor.

Omenn syndrome (OS) is a form of severe combined immunodeficiency (SCID), characterized by the occurrence of diffuse erythrodermia, hepatosplenomegaly, generalized lymphadenopathy, eosinophilia and highly elevated serum immunoglobulin (Ig) E level,[1] together with activated, autoreactive T lymphocyte infiltration of various organs. Most of these findings are observed soon after birth or during early infancy. Unless treated by allogeneic hematopoetic stem cell transplantation (SCT), the prognosis of OS is fatal.

Missense mutation in the recombination activating genes (*RAG)1* or *RAG2* and partial recombinase activity may result in OS.[1] These genes are also involved in the creation of various T cell repertoires. Total defect of enzymatic activity function causes SCID without producing mature lymphoid cells. Partial defect with leaky recombinase activity may lead to variable clinical features reflecting the actual degree of the enzyme defect. Indeed, our case showed an oligoclonal expansion of T lymphocytes with multiple second-site mutations leading to a typical OS with *RAG1*-deficient SCID.[2] In this report, we analyzed eosinophilia, eosinophil activity, and production of several cytokines in this syndrome.

Correspondence: Masahiko Kato, MD, Department of Allergy and Immunology, Gunma Children's Medical Center, 779 Shimohakoda, Hokkitsu-machi, Shibukawa, Gunma 377-8577, Japan. Email: mkato@gcmc.pref.gunma.jp

Received 29 August 2008; revised 28 September 2009; accepted 15 December 2009.

Case Report

We report the case of a 3-month-old boy presenting with generalized exudative erythrodermia, hepatosplenomegaly, draining otitis externa, and alopecia, with a history of *Pseudomonas aeruginosa* bacteremia requiring systemic antibiotic treatment. He was the second child of consanguineous parents with an older healthy daughter. Laboratory evaluation showed mild anemia, leukocytosis (104.0×10^9/L) with marked lymphocytosis (53.0×10^9/L) and eosinophilia (21.8×10^9/L), hypoalbuminemia (2.4 g/dL), and low serum Ig level (IgG 148 mg/dL; IgA < 1 mg/dL; IgM 2 mg/dL; IgE < 2 U/mL). Some eosinophils in both peripheral blood and bone marrow showed nuclear hypersegmentation such as three- or four-lobed nuclei (data not shown). Skin biopsy specimens showed lymphocytic invasion in the dermis, consistent with the graft-versus-host disease (GvHD) (data not shown). Immunophenotypic analysis showed the following percentages of lymphocyte subpopulations: cluster of differentiation (CD)3^+ 91.8%; $CD4^+$ 44.4%; $CD8^+$ 49.9%; $CD16^+$ 3.5%; $CD20^+$ < 0.1%; T cell receptor (TCR)$\gamma\delta^+$ 0.3%; human leukocyte antigen (HLA)-$DR^+/CD3^+$ 95.5%; $CD45RO^+/CD4^+$ 99.8%; and $CD45RO^+/CD8^+$ 97.0%. Analysis of T cell receptor Vβ repertoire in the periphery showed extremely restricted heterogeneity. There was no evidence of materno-fetal transplantation (MFT) from the results of HLA typing and fluorescent *in situ* hybridization analysis. Finally, mutation in *RAG1* was detected by DNA sequencing analysis.[2] Thus, a definitive diagnosis of OS was made, and immunosuppressive therapy with prednisolone (1.5 mg/kg/day) was started with the addition of cyclosporin

Table 1 Serum ECP and cytokine production in pre- and post-treatment of prednisolone (1.5 mg/kg/day)

	Pre-treatment	Day 7	Day 14	Day 21	Day 28	Disease control[†]
ECP (μg/L)[‡]	23.3	6.0	15.2	15.2	4.0	30.2 ± 4.4
IL-5 (pg/mL)[§]	5.0	2.2	2.9	0.8	4.1	9.6 ± 1.9
GM-CSF (pg/mL)	66.8	79.0	6.4	ND	6.4	126.6 ± 41.0
IL-4 (pg/mL)	78.9	41.8	12.2	ND	ND	26.2 ± 4.2
IL-13 (pg/mL)	99.8	14.6	19.1	6.6	11.2	5.1 ± 0.3
IL-10 (pg/mL)	7.7	4.6	5.1	6.3	10.2	28.9 ± 3.8
IFN-γ (pg/mL)	3.9	10.9	ND	ND	ND	114.7 ± 11.9
IL-2 (pg/mL)	ND	15.6	ND	ND	ND	14.9 ± 5.1

[†]Acute asthma (mean ± SEM, $n = 32$–75) as the disease control. [‡]ECP was determined using fluoro-immunoassay (Pharmacia-Upjohn, Uppsala, Sweden). [§]Cytokines were determined using the Bioplex Multiplex Human Cytokine Assay kit (Bio-Rad Laboratories, Hercules, CA, USA). ECP, eosinophil cationic protein; GM-CSF, granulocyte-macrophage colony-stimulating factor; IFN, interferon; IL, interleukin; ND, not detected.

A (9 mg/kg/day) to improve autoimmune manifestations. Four months after admission, the patient underwent allogeneic SCT with a full-matched unrelated cord blood unit, because a matched related donor was unavailable.[3] The conditioning regimen consisted of fludarabine at 25 mg/m^2 daily on days −7 to −3, melphalan at 70 mg/m^2 daily on days −4 to −3, and antithymocyte globulin at 10 mg/kg daily on days −2 and −1. The patient was treated with cyclosporin at 3 mg/kg and methylprednisolone at 1 mg/kg for GvHD prophylaxis. The total number of infused cells was 5.29×10^7/kg. The patient was successfully treated by altering the degree of immunosuppression and donor lymphocyte infusion (DLI) using donor cord-blood-derived activated CD4$^+$ T cells for mixed chimerism after unrelated cord-blood transplantation using reduced-intensity conditioning. Full donor chimerism in the bone marrow was also achieved on day +68.[3] Although the patient contracted mycobacterium avium complex infection, anti-mycobacterium therapy using ethambutol, rifampin, and azithromycin, prevented recurrence of high fever and produced a stable state after transplantation.

We analyzed eosinophilia, eosinophil activity, and production of several cytokines in this syndrome. Although our case before prednisolone (1.5 mg/kg/day) treatment presented with marked hypereosinophilia (21 800/μL) almost 50 times higher than that in disease control, namely, acute asthma (4.0 ± 0.4 years old), the eosinophil cationic protein (ECP) level was almost comparable to that of acute asthma (eosinophil counts, 21 800 vs 442.3 ± 70.0/μL; ECP levels, 23.3 vs 30.2 ± 4.4 ng/mL), as shown in Table 1. Figure 1 shows that the expression of CD69, an activation marker of eosinophils,[4] on peripheral eosinophils in our case was minimal compared with a patient with severe atopic dermatitis as positive control. Serum concentrations of T helper (Th)2 cytokines including interleukin (IL)-4 and IL-13 before treatment were markedly elevated compared with those of acute asthma (IL-4, 78.9 vs 26.2 ± 4.2; IL-13, 99.8 vs 5.1 ± 0.8 pg/mL). In contrast, the concentrations of the eosinophil-active cytokines IL-5 and granulocyte-macrophage colony-stimulating factor (GM-CSF) were not very high compared with those of acute asthma (IL-5, 5.0 vs 9.6 ± 1.9 pg/mL; GM-CSF, 66.8 vs 126.6 ± 41.0 pg/mL). The concentrations of the Th1 cytokines interferon (IFN)-γ and IL-2 were not elevated. After the treatment, the concentrations of Th2 cytokines decreased, whereas those of Th1 cytokines transiently increased. As shown in Table 2, when peripheral blood

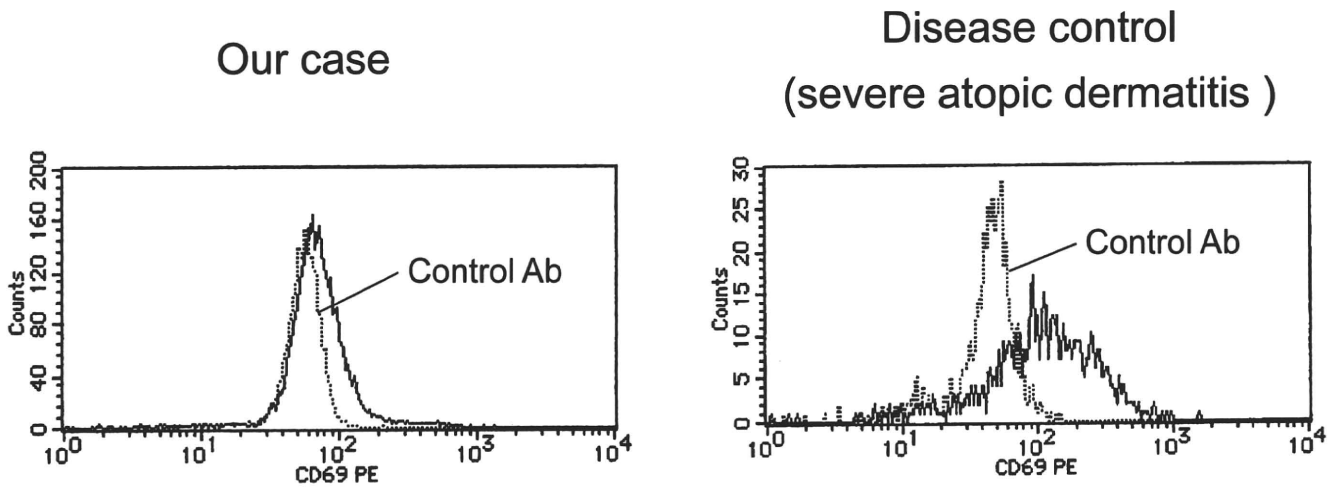

Fig. 1 Surface expression of cluster of differentiation (CD)69 antigen in eosinophils. Expression of CD69 in peripheral blood eosinophils in our case and that in a disease control were determined by flow cytometry and compared with that of an isotype-matched control antibody. Disease control represented a patient with severe atopic dermatitis (5 months, male). He also showed peripheral blood eosinophilia (21 762/μL) and highly elevated serum immunoglobulin E (17 867 IU/mL). Ab, antibody.

Table 2 Cytokine production in the peripheral mononuclear leukocytes

	IL-5	IL-4	IL-13	IFN-γ	IL-2
Pre-treatment	21.4†	1476.9	5201.0	6664.9	4372.6
Day 7 of treatment‡	7.2	43.8	302.0	792.7	4787.8
Day 14 of treatment‡	12.3	27.2	4.0	7.8	7.9

†pg/mL. ‡Prednisolone (1.5 mg/kg/day). The cells stimulated by phorbol 12-myristate 13-acetate and ionomycin for 24 h. IFN, interferon; IL, interleukin.

mononuclear cells (PBMC) from the patient were stimulated with phorbol 12-myristate 13-acetate (PMA) and ionomycin for 24 h,[5] the concentrations of IL-4, IL-13, IFN-γ and IL-2 markedly increased; however, that of IL-5 was not so high compared with that of acute asthma (IL-5, 21.4 vs 37.6 ± 7.1 pg/mL). The capacity to produce these cytokines was diminished after immunosuppressive therapy.

Discussion

We measured the serum level of ECP, a marker of eosinophil activation, and found that its level was not so high, suggesting that despite the prominent eosinophilia, marked activation of eosinophils was not observed in our case. The amount of ECP released in cell culture from hypereosinophilic syndrome (HES) patients is higher than that in those with other hypereosinophilic conditions (including OS); therefore, eosinophils in HES are more aggressive toward tissues than those in other conditions.[6] These results were also supported by the finding that the upregulation of CD69, an activated surface marker of eosinophils, on peripheral eosinophils is minimal compared with that in patients with atopic dermatitis. Secondly, we investigated cytokine profiles in both serum and PBMC from our patient. Th2-type lymphocytes might be activated because of eosinophilia and elevated IgE concentration in typical OS. However, reports on cytokine production in OS remain controversial. For example, *in vitro* stimulation of lymphocytes from an OS patient induced IL-4 and IL-5 secretion in the serum,[7] while others showed high concentrations of serum IL-5 in OS.[8] In contrast, other investigators failed to detect Th2 cytokines (IL-4, IL-5, and IL-13), but detected Th1 cytokines (tumor necrosis factor [TNF]-α, IFN-γ, and IL-1β) in an OS patient with reverse transcription–polymerase chain reaction (RT–PCR) for cytokine mRNA expression.[9] Our case showed high concentrations of Th2 cytokines, especially IL-4 and IL-13, in both serum and PBMC, but serum IL-5 concentration was not very high. In OS, oligoclonal expansion of T lymphocyte induces Th1/Th2 cytokine paradigm. Thus, regulations of cytokine production appear to be different depending on each case. In fact, not all OS cases show hypereosinophilia. On the other hand, marked eosinophilia can be induced without eosinophilic activation.

How can we explain an atypical cytokine profile and discrepancies between marked eosinophilia and less eosinophil activation? Accumulating evidence suggests that eosinophil differentiation and infiltration are regulated by IL-5, GM-CSF and IL-13, while eosinophil effector functions, such as degranulation, are regulated by IL-5 and GM-CSF but not by IL-13.[10–12] Thus, discrepancies between marked eosinophilia and less eosinophil activation in the present case might be explained, at least in part, by the atypical cytokine profile where IL-13 concentration is markedly elevated but that of IL-5 and GM-CSF were not in this patient. Another possible reason is that our case showed oligoclonal expansion of T lymphocytes with multiple second-site mutations leading to typical OS with *RAG1*-deficient SCID.[2,13] The patient is homozygous for a single-base C deletion predicted to cause frameshift mutation and premature termination of *RAG1*. Six compensatory second-site mutations were found in revertant T cells, showing an activated phenotype with a restricted TCR repertoire, expanding in peripheral blood, and possibly contributing to the modification of his clinical features, suggesting that revertant T-cell mosaicism is responsible for OS phenotypes switching from T-B-SCID.[13] In contrast, we speculate that *RAG1* activity in this patient is completely defective in B cells as well as granulocytes, reflecting the impaired B-cell differentiation.[2] Thus, it is suggested that the production of IgE was undetectable, although the production of IL-4 and IL-13 was increased in this patient. Therefore our patient may not show typical cytokine production and hyper IgE, even though he showed typical clinical features of OS.

Although the detailed mechanisms of eosinophilia, minimal activation of eosinophils and atypical cytokine profile were not completely clarified in this case, the mechanism of eosinophil proliferation might be different from that of eosinophil activation and an appropriate balance of cytokine production might be involved in this reaction.

Acknowledgments

This study was approved by the Ethics Committee of Gunma Children's Medical Center. We wish to thank Takafumi Yamaguchi for his editorial support.

References

1 Villa A, Santagata S, Bozzi F *et al.* Partial V(D)J recombination activity leads to Omenn syndrome. *Cell* 1998; **93**: 885–96.
2 Wada T, Toma T, Okamoto H *et al.* Oligoclonal expansion of T lymphocytes with multiple second-site mutations leads to Omenn syndrome in a patient with *RAG1*-deficient severe combined immunodeficiency. *Blood* 2005; **106**: 2099–101.
3 Tomizawa D, Aoki Y, Nagasawa M *et al.* Novel adopted immunotherapy for mixed chimerism after unrelated cord blood transplantation in Omenn syndrome. *Eur. J. Heamatol.* 2005; **75**: 441–4.
4 Toma T, Mizuno K, Okamoto H *et al.* Expansion of activated eosinophils in infants with severe atopic dermatitis. *Pediatr. Int.* 2005; **47**: 32–8.
5 Hashimoto T, Akiyama K, Kawaguchi H *et al.* Correlation of allergen-induced IL-5 and IL-13 production by peripheral blood T cells of asthma patients. *Int. Arch. Allergy Immunol.* 2004; **134**(Suppl. 1): 7–11.
6 Bobbio-Pallavicini E, Confalonieri M, Tacconi F *et al.* Study of release of eosinophil cationic proteins (ECP and EPX) in the hypereosinophilic syndrome (HES) and other hypereosinophilic conditions. *Panminerva Med.* 1998; **40**: 186–90.
7 Schandené L, Ferster A, Mascart-Lemone F *et al.* T helper type 2-like cells and therapeutic effects of interferon-γ in

combined immunodeficiency with hypereosinophilia (Omenn's syndrome). *Eur. J. Immunol.* 1993; **23**: 56–60.
8 Melamed I, Cohen A, Roifman CM. Expansion of CD3+CD4-CD8-T cell population expressing high levels of IL-5 in Omenn's syndrome. *Clin. Exp. Immunol.* 1994; **95**: 14–21.
9 Harville TO, Adams DM, Howard TA *et al.* Oligoclonal expansion of CD45RO+ T lymphocytes in Omenn syndrome. *J. Clin. Immunol.* 1997; **17**: 322–32.
10 Weller PF. Cytokine regulation of eosinophil function. *Clin. Immunol. Immunopathol.* 1992; **62**: S55–9.
11 Horie S, Gleich GJ, Kita H. Cytokines directly induce degranulation and superoxide production from human eosinophils. *J. Allergy Clin. Immunol.* 1996; **98**: 371–81.
12 Horie S, Okubo Y, Hossain M *et al.* Interleukin-13 but not interleukin-4 prolongs eosinophil survival and induces eosinophil chemotaxis. *Intern. Med.* 1997; **36**: 179–85.
13 Kato M, Kimura H, Seki M *et al.* Omenn syndrome-review of several phenotypes of Omenn syndrome and *RAG1/RAG2* mutations in Japan. *Allergol. Int.* 2006; **55**: 115–9.

Eur J Pediatr (2010) 169:839–844
DOI 10.1007/s00431-009-1126-6

ORIGINAL PAPER

Successful cord blood transplantation for a CHARGE syndrome with *CHD7* mutation showing DiGeorge sequence including hypoparathyroidism

Hirosuke Inoue · Hidetoshi Takada · Takeshi Kusuda · Takako Goto · Masayuki Ochiai · Tadamune Kinjo · Jun Muneuchi · Yasushi Takahata · Naomi Takahashi · Tomohiro Morio · Kenjiro Kosaki · Toshiro Hara

Received: 22 July 2009 / Accepted: 1 December 2009 / Published online: 6 January 2010

Abstract It is rare that coloboma, heart anomalies, choanal atresia, retarded growth and development, and genital and ear anomalies (CHARGE) syndrome patients have DiGeorge sequence showing severe immunodeficiency due to the defect of the thymus. Although the only treatment to achieve immunological recovery for these patients in countries where thymic transplantation is not ethically approved would be hematopoietic cell transplantation, long-term survival has not been obtained in most patients. On the other hand, it is still not clarified whether hypoparathyroidism is one of the manifestations of CHARGE syndrome. We observed a CHARGE syndrome patient with chromodomain helicase DNA-binding protein 7 mutation showing DiGeorge sequence including the defect of T cells accompanied with the aplasia of the thymus, severe hypoparathyroidism, and conotruncal cardiac anomaly. He received unrelated cord blood transplantation without conditioning at 4 months of age. Recovery of T cell number and of proliferative response against mitogens was achieved by peripheral expansion of mature T cells in cord blood without thymic output. Although he is still suffering from severe hypoparathyroidism, he is alive without serious infections for 10 months.

Keywords CHARGE syndrome · DiGeorge sequence · *CHD7* mutation · Hypoparathyroidism · Cord blood transplantation

Abbreviations

CHD7	Chromodomain helicase DNA-binding protein 7
CBT	Cord blood transplantation
TCR	T cell receptor
PHA	Phytohemagglutinin
Con A	Concanavalin A
ABR	Auditory brainstem response
GVHD	Graft versus host disease

Introduction

Coloboma, heart anomalies, choanal atresia, retarded growth and development, and genital and ear anomalies (CHARGE) syndrome is a distinctive clinical entity with multiple congenital anomalies [12]. Mutations in the gene chromodomain helicase DNA-binding protein 7 (*CHD7*) were identified as a cause of CHARGE syndrome [25]. *CHD7* on chromosome 8 (8q12.1) is a member of the chromodomain helicase DNA binding domain family [25]. Chromatin remodeling is a recognized mechanism of gene expression regulation, and the *CHD7* gene is likely to play a significant role in embryonic development and cell cycle regulation [29]. CHD7 is expressed throughout the neural crest containing mesenchyme of the pharyngeal arches. Mouse embryo at 10.5 days postcoitum expressed *Chd7* in

H. Inoue · H. Takada (✉) · T. Kusuda · T. Goto · M. Ochiai · T. Kinjo · J. Muneuchi · Y. Takahata · T. Hara
Department of Pediatrics, Graduate School of Medical Sciences, Kyushu University,
3-1-1 Maidashi, Higashi-ku,
Fukuoka 812-8582, Japan
e-mail: takadah@pediatr.med.kyushu-u.ac.jp

N. Takahashi · T. Morio
Department of Pediatrics and Developmental Biology, Graduate School of Medical and Dental Sciences, Tokyo Medical and Dental University, Tokyo, Japan

K. Kosaki
Department of Pediatrics, School of Medicine, Keio University, Tokyo, Japan

the cardiac outflow tract, truncus arteriosus, facio-acoustic preganglion complex, hindbrain, forebrain, mandibular component of the first branchial arch, otic vesicle, optic stalk/optic vesicle, and olfactory pit [12]. Thus, CHARGE syndrome has the potential of multiple presentations.

Cellular immunodeficiency due to the lack of the thymus is not widely recognized as a manifestation of CHARGE syndrome. Recently, severe hypoparathyroidism and conotruncal cardiac anomaly were reported in patients with CHARGE syndrome caused by *CHD7* mutations having DiGeorge sequence characterized by the defect of T cells accompanied by thymus aplasia [21, 28, 30]. Although thymus hypoplasia or agenesis is rare in postnatal CHARGE syndrome cases [3], Sanlaville et al. reported that it was observed in seven of ten CHARGE syndrome fetuses [22]. Recently, Jyonouchi et al. reported that 8% (two of 25) of CHARGE syndrome patients had a phenotype of severe combined immunodeficiency with defect of T cells [10]. On the other hand, it is still not clarified whether hypoparathyroidism is one of the manifestations of CHARGE syndrome since only three CHARGE syndrome patients with *CHD7* mutation were reported to have hypoparathyroidism [21, 28, 30]. It is suggested that neural crest defect underlies the clinical overlap of both chromosome 22q11 deletion and CHARGE syndrome [22]. Accordingly, a case manifesting the CHARGE syndrome with deletion in chromosome 22q11 was reported [7].

Here, we report a patient with CHARGE syndrome with a *CHD7* mutation, who had severe T cell immune deficiencies due to thymic aplasia, severe limb anomalies, and congenital hypoparathyroidism. He was successfully treated with cord blood transplantation (CBT).

Case report

The patient was born at 39 weeks of gestational age. His birth weight was 2,488 g. Cardiac anomaly and polyhydramnion were detected by fetal ultrasound examination during his late prenatal period. Karyotype analysis of amniotic fluid showed 46,XY. His family members were healthy without having even minor anomalies.

Shortly after birth, he was admitted to the neonatal intensive care unit (NICU) in Kyushu University Hospital. He showed the characteristic facial features such as a hypertelorism and unilateral facial palsy (Fig. 1a), asymmetry of ears with protruding, helix hypoplasia, low-set and square-shaped right ear, absent anthelix, low-set left ear (Fig. 1b, c), and bilateral coloboma of the choroid. In addition, thumb polydactyly and cleft of the right hand and cleft and cutaneous syndactyly of the bilateral feet were observed (Fig. 1d–g). He had no genital abnormalities. Hematological examinations revealed white blood cell count of 4,330/μl with severe lymphopenia (neutrophils 68.5%, lymphocytes 7%, monocytes 18%). Serum calcium, phosphorus, and parathyroid hormone levels were 7.8 mg/dl, 8.4 mg/dl, and 4.5 pg/ml, respectively, showing hypoparathyroidism. Serum thyroid hormone levels were normal. Lymphocyte surface marker analysis by a flow cytometer revealed a marked decrease of T lymphocytes: $CD3^+$ 2.8% (8 cells/μl), $CD4^+$ 2.3% (7 cells/μl), and $CD8^+$ 15.3% (46 cells/μl; Table 1). T cell receptor (TCR) $\gamma\delta^+$ cells, $CD16^+/CD56^+$ cells, and $CD19^+$ cells were 0.1%, 35.9%, and 52.9%, respectively. Proliferative response of mononuclear cells against phytohemagglutinin (PHA) and concanavalin A (Con A) was 123 %S.I. (normal controls; 254–388) and 2,530 cpm (20,300–65,700), respectively. Analysis of the TCRVβ repertoire showed an abnormal pattern with overexpansion of $V\beta21.3^+$ cells (20.9%; Fig. 2a). Serum IgG, IgA, and IgM concentrations were 899, 5, and 19 mg/dl, respectively. Fluorescent in situ hybridization analysis revealed a lack of maternal cell engraftment in peripheral blood and no deletion at 22q11.2.

Computed tomography and fiberoptic laryngoscope examination revealed left choanal atresia with posterior choanal stenosis and laryngomalacia, respectively. Auditory brainstem response revealed bilateral severe sensorineuronal hearing loss. An echocardiogram and chest computed tomography scan revealed truncus arteriosus (Van Praagh type A4) and interruption of aortic arch (type B) with aberrant right subclavian artery. At 14 days of age, he underwent bilateral pulmonary artery banding operation because he was too small to receive the radical correction of truncus arteriosus and interruption of aortic arch at that time. Thymus was not detected at the time of operation.

Thus, we made the clinical diagnosis of CHARGE syndrome with manifestations of complete-type athymic DiGeorge sequence. The *CHD7* gene of the patient was analyzed according to the method described previously [2], and heterozygous c.1036A > T (R346X) mutation was observed in exon 2. He received unrelated CBT without conditioning at 4 months of age (Fig. 2b). Human leukocyte antigen full-matched female cord blood cells (28.03×10^7 cells/kg) were infused. FK506 and short-term methotrexate were used for graft versus host disease (GVHD) prophylaxis. He had only mild skin manifestation of GVHD, which resolved by prednisolone (1 mg/kg/day). On day 25 after CBT, $CD3^+$ cells increased to 60.1% of lymphocytes (1,471 cells/μl), 93.8% of which were positive for CD45RO. Analysis of the TCRVβ repertoire on day 27 showed an abnormal pattern with overexpansion of $V\beta16^+$ cells (7.3%) and $V\beta17^+$ cells (9.7%), and a different profile was observed between pre-CBT and post-CBT (Fig. 2a). Proliferative response to Con A and PHA normalized on day 50 (20,500 cpm) and on day 174 (284 %S.I.), respectively. Chimerism analysis on day 173 showed that most of the $CD3^+$

Fig. 1 Clinical manifestations of the patients. **a** Frontal view of the face showing hypertelorism and right facial palsy. **b** Lateral view of the right ear showing protruding, helix hypoplasia, and low-set ear. **c** Lateral view of the left ear showing square-shaped, absent anthelix, and low-set ear. Note asymmetry of ears. **d** Thumb polydactyly and cleft of the right hand. **e** Normal left hand. **f, g** Cleft and cutaneous syndactyly of the bilateral foots. Written consent was obtained for publication of these pictures

cells were of donor origin (94.5% of $CD3^+$ cells were XX, 5.5% were XY). At 10 months of age (day 169 after CBT), $CD3^+$ cells were 36.3% of lymphocytes (973 cells/μl), and 86.2% of T cells were positive for CD45RO. T cell receptor excision circles were below the detection limit before CBT, confirming the lack of thymic output (data not shown).

He is alive without serious infections with regular administration of immunoglobulin and prophylactic antibiotics. At 10 months of age, serum calcium, phosphorus, and parathyroid hormone levels are 7.2 mg/dl, 6.1 mg/dl, and 3.0 pg/ml, respectively. He is still receiving calcium preparation and alfacalcidol.

Table 1 Immunological studies

	Pretransplantation	Posttransplantation
$CD3^+$ cells (% lymphocytes)	2.8	36.3
$CD3^+$ cells (cells/μl)	8	973
$CD45RO^+/CD3^+$ (%)	87.7	86.2
$CD45RO^-/CD3^+$ (%)	12.4	10.9
$CD4^+$ cells (% lymphocytes)	2.3	24.2
$CD4^+$ cells (cells/μl)	7	648
$CD8^+$ cells (% lymphocytes)	15.3	12.1
$CD8^+$ cells (cells/μl)	46	324
TCR $\gamma\delta^+$ (%)	0.1	0.2
$CD19^+$ (%)	52.9	33.3
$CD16^+/CD56^+$ (%)	35.9	29.7
Proliferative response		
Against PHA (%S.I.)	123	284
Against Con A (cpm)	2,530	20,500
IgG (mg/dl)	899	425
IgM (mg/dl)	19	83
IgA (mg/dl)	5	66
Karyotype of $CD3^+$ cells	99.5% of 46,XY	5.5% of 46,XY
	0.5% of 46,XX	94.5% of 46,XX

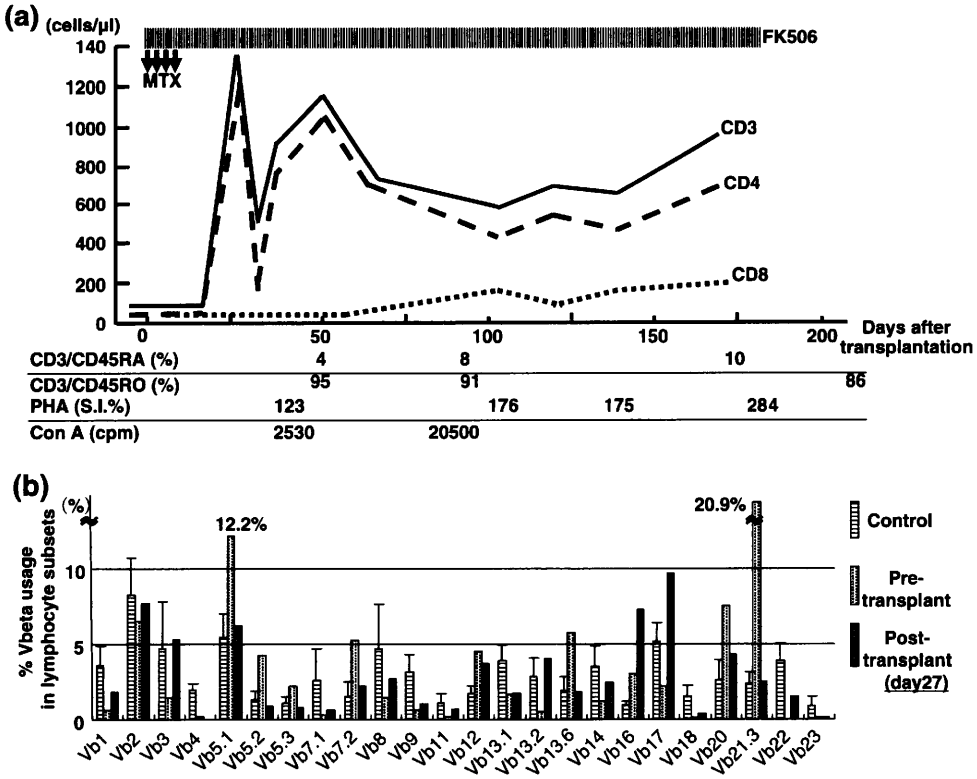

Fig. 2 Clinical course and immunological recovery after the cord blood transplantation. **a** Clinical course of the cord blood transplantation. *MTX* methotrexate, *PHA* phytohemagglutinin, *Con A* concanavalin A. **b** TCRVβ repertoire profile on the patient and control subjects. Note the skewing in the TCR repertoire before and after transplantation. *TCR* T cell receptor

Discussion

Our patient showed absence of T lymphocytes accompanied with aplasia of the thymus manifesting complete-type DiGeorge sequence, a rare complication of CHARGE syndrome [1, 30]. T cell number of the patient was recovered by CBT, although most of the T cells showed memory phenotype reflecting peripheral expansion of donor cord blood-derived mature T cells and the lack of the thymic output. He presented with additional rare manifestations, severe limb anomalies, and congenital hypoparathyroidism. DiGeorge sequence is associated with a deletion of chromosome 22q11.2 in approximately 80% of patients [23]. Interestingly, Markert et al. reported that only 52% of 54 patients with DiGeorge sequence had a deletion of 22q11, and 26% had CHARGE phenotype without the deletion [15]. A number of genes have been identified in the 22q11.2 region [31], including *TBX1* that is a major genetic determinant of del22q11.2 syndrome. As TBX1 is a transcription factor that contains a DNA binding domain, it is possible that TBX1 is a functional target for CHD7.

Thymic hypo/agenesis was observed in 70% of fetuses with CHARGE syndrome [22]. The high frequency of thymic defect in fetuses suggests that accompanying immune deficiency may be more common in this disease than previously reported. It is possible that many of athymic patients were counted on DiGeorge syndrome, rather than CHARGE syndrome. Otherwise, CHARGE syndrome patients with thymic defect may more often die during perinatal period because of the immunodeficiency or other accompanying anomalies such as severe cardiac defect. Although there have been a few reports of stem cell transplantation for the treatment of T cell deficiency in complete-type DiGeorge sequence, this is the first case of CBT for the treatment of CHARGE syndrome with *CHD7* mutation manifesting T cell defect [8, 14, 18]. The optimal treatment for patients with complete-type DiGeorge sequence has not been established. In the absence of treatment, patients usually die in the first 2 years of life [16]. Therefore, prompt reconstitution of the immune function is required to prevent fatal infectious complications. The common treatments for immunological reconstitution in complete-type DiGeorge sequence are thymic and bone marrow transplantation [13, 15]. Although thymic transplantation would be more reasonable from the physiological point of view, it is not ethically approved in Japan. We selected CBT without conditioning regimen for our patient because of the following reasons: (1) lack of sibling donors, (2) more noninvasive procurement and more rapid availability than the matched unrelated donors, (3) lower risk of GVHD or viral transmission in CBT compared with bone marrow or peripheral blood stem cells [5], and (4) higher frequency of naïve T cells in cord blood [6], which have a longer lifespan than their memory counterparts [26]. Because of the lack of thymic output after the transplantation in this disease, the high frequency of naïve T cells in the donor cells may be an important factor to avoid early immune senescence. On the other hand, it may take more time for the recovery of neutrophils in CBT leaving a higher risk of infection compared with bone marrow or peripheral stem cell transplantation [5]. In addition, naïve T cells in cord blood may require a longer time to mature into effecter memory cells and thus do not provide immediate defense against microbial agents [11]. Our patient received CBT in the NICU and has been bred in a closed infant incubator since birth. This might in part contribute to the decrease of the risk of infections and to the success of CBT.

Ryan et al. [20] reported that only a few patients (1–4%) had mild limb abnormalities in 548 patients with chromosome 22q11 deletions. Limb anomalies were not initially described in CHARGE syndrome [4]. Recently, limb anomalies have been reported as a rare manifestation in CHARGE syndrome [3, 17, 19]. On the other hand, Brock et al. [4] reported that limb anomalies occurred in about 30% of patients with definite or probable CHARGE syndrome. It is interesting that limb anomalies with DiGeorge sequence are more frequently observed in male (P value <0.034), and limb anomalies were observed in 70.0% of male DiGeorge sequence with definite CHARGE syndrome [4]. Williams proposed that CHARGE syndrome is caused by a disruption of mesenchymal–epithelial (including ectoderm and endoderm) interaction [27]. Sanlaville et al. [22] showed that the *CHD7* gene is also expressed in the limb bud mesenchyme during embryogenesis. Van de Laar et al. [24] reported that three CHARGE syndrome patients with CHD7 mutation had severe limb anomalies. Therefore, it is possible that *CHD7* mutation itself is responsible for limb defects, and limb anomalies are more strongly associated with *CHD7* mutation than 22q11 deletion.

In patients with 22q11 deletion, 203 of 340 (60%) had hypoparathyroidism and hypocalcaemia, and the hypocalcaemia resolved in 70% [20]. On the other hand, only three CHARGE syndrome patients with *CHD7* mutations had hypoparathyroidism [21, 28, 30]. It is interesting that the three patients had severe T cell deficiency [21, 28, 30]. As TBX1 might be a functional target of CHD7, it is possible that hypoparathyroidism may be more common in CHARGE syndrome than previously recognized. Günther et al. showed by using *glial cells missing2*-deficient mice that thymus had a backup mechanism of parathyroid gland and thymus itself secreted parathyroid hormone when parathyroid glands was absent [9]. It is possible that intractable hypocalcemia continues when both parathyroid gland and thymus are absent.